

Anatomical Methods for Voxellation of the Mammalian Brain*

Daniel M. Sforza,^{1,2} Jacopo Annese,³ Dahai Liu,^{1,2} Shawn Levy,⁴ Arthur W. Toga,³ and Desmond J. Smith^{1,2,5}

(Accepted October 1, 2003)

Voxelation allows high-throughput acquisition of three-dimensional gene expression patterns in the brain through analysis of spatially registered voxels (cubes). The method results in multiple volumetric maps of gene expression analogous to the images reconstructed in biomedical imaging techniques. An important issue for voxelation is the development of approaches to anchor correctly harvested voxels to the underlying anatomy. Here, we describe experiments to identify fixation and cryopreservation protocols for improved registration of harvested voxels with neuroanatomical structures. Paraformaldehyde fixation greatly reduced RNA recovery as judged by ribosomal RNA abundance. However, gene expression signals from paraformaldehyde-fixed samples were not appreciably diminished as judged by average signal–noise ratios from microarrays, highlighting the difficulties of accurate quantitation of cross-linked RNA. Additional use of cryoprotection helped to improve further RNA recovery and signal from fixed tissue. It appears that the best protocol to provide the necessary resolution of neuroanatomical information in voxelation entails a controlled dose of fixation and thorough cryoprotection, complemented by histological staining.

KEY WORDS: Cryoprotection; fixation; microarrays; paraformaldehyde; voxelation.

INTRODUCTION

Genome-wide acquisition and analysis of gene expression patterns will be a necessary informational infrastructure for understanding of the brain at the molecular

level. The advent of microarray technology renders this goal feasible. One recently developed approach for genome-scale acquisition of brain gene expression patterns employs microarray analysis of spatially registered voxels (cubes) harvested from the brain (1,2). The method is called voxelation and results in multiple volumetric maps of gene expression analogous to the images reconstructed in biomedical imaging techniques, such as computed tomography (CT), positron emission tomography (PET), and magnetic resonance imaging (MRI).

Voxelation has been employed to analyze gene expression patterns from the human and rodent brain (3–6). The human studies examined both normal brains and those from individuals with Alzheimer's disease (4), whereas the mouse studies investigated the normal brain and brains from mice in which a model of Parkinson's disease had been induced using toxic doses of methamphetamine (3). These studies yielded large amounts of data, and a number of analytical techniques were employed to extract insights

* Special issue on Expression Profiling Within the Central Nervous System II.

¹ Department of Molecular and Medical Pharmacology, School of Medicine, University of California, Los Angeles, California.

² Crump Institute for Molecular Imaging, School of Medicine, University of California, Los Angeles, California.

³ Laboratory of Neuro Imaging, Department of Neurology, School of Medicine, University of California, Los Angeles, California.

⁴ Department of Molecular Physiology and Biophysics, Vanderbilt University Medical Center, Nashville, Tennessee.

⁵ Address reprint requests to: Desmond J. Smith, Department of Molecular and Medical Pharmacology, UCLA School of Medicine, 23-120 CHS, Box 951735, Los Angeles, California 90095-1735. Tel: 310-206-0086; Fax: 310-825-6267; E-mail: DSmith@mednet.ucla.edu

from the data. Clusters of genes were identified with correlated expression patterns, as well as genes that differed significantly between control and experimental samples across all voxels. In addition to these analyses, singular value decomposition was also employed. This mathematical technique is an exploratory approach that relies on no pre-existing hypotheses or notions concerning the data. Singular value decomposition identified clusters of genes (gene "vectors") that most efficiently explained the variance in the data. These gene vectors showed interesting regional patterns of expression, and their associated genes may play an important role in differentiation of the mouse and human brain (3,4). In addition, singular value decomposition identified a gene vector that showed a significant spatial shift away from the striatum in the normal mouse brain toward the hippocampus in the Parkinson's brain (3). These results suggest that high-throughput acquisition of gene expression patterns in combination with singular value decomposition has the potential to identify functionally abnormal neuroanatomical regions in neurological disease states. The use of analysis of variance (ANOVA) was found to produce results consistent with those from singular value decomposition (5).

The initial voxelation studies of the human brain employed a resolution of approximately 1 cm³ (4), whereas the studies of the rodent brain employed an average volumetric resolution of 7.5 μ l. To obtain higher resolution voxelation images of gene expression for the human and rodent brain, instrumentation is required to allow spatially registered harvesting of miniaturized voxels. Two such devices have been constructed; the instrument for the human brain results in voxels of size 87 μ l, whereas the instrument for the rodent brain results in voxels of 1 μ l (6).

The voxelation approach is facilitated by a precise anatomical characterization of harvested voxels. To date, voxelation studies have used fresh tissue slabs, but a drawback of this approach is the deformation of the tissue during the process of physical voxelation, which can hinder registration of voxels to the underlying neuroanatomy. Although this is not a major problem for low-resolution studies, it becomes a significant factor at higher resolution.

The process of fixation improves tissue resilience, and it is a prerequisite for morphologically accurate neuroanatomical maps produced by sectioning and histological staining (7). Cryopreservation is also necessary if histological sections are harvested from frozen specimens (8); this technique favors RNA preservation as it circumvents treatment with chemical solvents. The introduction of fixation and cryopreservation protocols should therefore improve the resolution of the voxelation technique and help provide a very detailed neuroanatomical reference system for the localization of gene expression.

In this report, we describe experiments to evaluate the utility of paraformaldehyde fixation and cryopreservation using graded solutions of sucrose in order to improve the registration of brain gene expression images obtained through voxelation with the neuroanatomy.

EXPERIMENTAL PROCEDURE

Perfusion Protocol. Adult C57BL/6J male mice (10 to 24 weeks, 25 to 31 g) underwent intracardiac perfusion under deep halothane anesthesia. For each animal, the vasculature was cleared with 11–22 ml of ice-cold phosphate-buffered saline (PBS) solution. Various perfusion protocols were then applied in order to test the effect of 4% paraformaldehyde and graded sucrose solutions on the quality of RNA recovered from brain tissue.

In the control condition, the perfusion was limited to PBS solution (condition 1). In the next condition (cryoprotected; condition 2), mice were additionally perfused with 67 ml of 10%, 20%, and 30% ice-cold phosphate-buffered sucrose solutions (pH 7.4). The sucrose solutions were each perfused for 45 min. In the next experimental condition (fixed; condition 3), in addition to the PBS perfusion, 67 ml of 4% paraformaldehyde in PBS (pH 7.4) was perfused for a period of 45 min. In the last condition (fixed and cryoprotected; condition 4), fixation and cryoprotection were combined; that is, perfusion with PBS was followed by 4% paraformaldehyde and then graded solutions of sucrose, as described above. This complete protocol lasted approximately 190 min. All investigated conditions are summarized in Table I.

After perfusion, brains were removed from the skull and the hemispheres separated and immediately frozen in chilled isopentane. Tissue blocks were kept at -70°C before RNA testing and histological processing.

Electropherogram. Total RNA quality was assessed by microcapillary electrophoresis using the Agilent BioAnalyzer 2100 (Agilent Technologies, Palo Alto, CA, USA). Evaluation of 18S and 28S RNA peaks and background noise were employed for this purpose.

Microarrays. Microarrays containing 22,172 cloned genes from the National Institute on Aging 15k cDNA clone set, mouse sequence-verified clones from Research Genetics, and several control genes were generated by the Vanderbilt Microarray Shared Resource (VMSR). Full gene lists and protocols are available at <http://array.mc.vanderbilt.edu>. Briefly, all cDNA clones were amplified (9) and verified by gel electrophoresis. The dried polymerase chain reaction (PCR) products were then resuspended in 40 μ l

Table I. Volume of Solutions Perfused in Each Condition

Condition	Saline* (ml)	Fixation [†] (ml)	Cryoprotection [‡] (ml)
1	11–22	—	—
2	11–22	—	67
3	11–22	67	—
4	11–22	67	67

* Ice-cold phosphate-buffered saline (PBS).

[†] 4% paraformaldehyde in PBS (pH 7.4).

[‡] Each of 10%, 20%, and 30% ice-cold phosphate-buffered sucrose solutions (pH 7.4).

VMSR buffer A (Vanderbilt Microarray Shared Resource, Nashville, TN, USA) resulting in an average concentration of 400–700 $\mu\text{g ml}^{-1}$ per product. The PCR products were then transposed to 384-well plates and robotically arrayed using a BioRobotics MicroGrid II microarray printing robot (Apogent Discoveries, Hudson, NH, USA) onto polylysine-coated glass slides (Cel Associates, Pearland, TX, USA). The microarrays were cross-linked using 80 mJ of ultraviolet energy (Stratgene Stratalink, La Jolla, CA, USA). After cross-linking, the arrays were baked for 2 h at 70°C in a standard oven and stored under low humidity conditions until use.

RNA Isolation, Labeling, and Hybridization. Total RNA was isolated using the RNeasy Lipid Tissue Mini Kit column (Qiagen, Hilden, Germany). Frozen samples were placed in QIAzol Lysis Reagent (Qiagen) and homogenized using a Tissue-Tearor homogenizer (BioSpec Products, Bartlesville, OK, USA). Subsequent steps were done according to the manufacturer's instructions. To produce targets for hybridization to the cDNA microarrays, 10 μg of total RNA was labeled with fluorescent nucleotides by chemical coupling after reverse transcription. The total RNA was mixed with 6 μg of anchored oligo-dT (5'-TTTTTTTTTTTTTTTTT VN-3') and incubated at 70°C for 10 min followed by 10 min at 4°C in a total volume of 18 μl . The denatured and annealed RNA was then reverse transcribed in a 30- μl reaction mix containing reaction buffer (50 mM Tris-HCl, 75 mM KCl, 3 mM MgCl_2 , pH 8.3), 10 mM dithio-threitol, 200 μM dATP, dGTP, dCTP, 51 μM dTTP, 149 μM amino-allyl-UTP (Sigma, St. Louis, MO, USA), and 200 U SuperScriptII reverse transcriptase (Life Technologies, Gaithersburg, MD, USA). The reactions were incubated at 42°C for 2 h. After incubation, 10 μl of 1 M NaOH and 10 μl of 0.5 M EDTA was added to degrade the remaining template RNA and the samples incubated at 70°C for 10 min. The reaction was neutralized by the addition of 10 μl of 1 M HCl followed by 300 μl of Qiagen Buffer PB (PCR Cleanup kit, Qiagen, Valencia, CA, USA). Reactions were purified using Qiagen's PCR cleanup kit following the manufacturer's directions with the substitution of 80% ethanol for Qiagen's PE buffer and water for Qiagen's EB buffer. Following purification, individual samples were desiccated, resuspended in 7 μl 0.1 M sodium bicarbonate buffer, and chemically coupled to monofunctional reactive cyanine dyes (Amersham Biosciences, Buckinghamshire England). Unbound cyanine dyes were removed by purification with Qiagen's PCR cleanup kit as described above. After purification, the labeled samples were combined to Cy3-Cy5 pairs, desiccated, and resuspended in 100 μl hybridization buffer (25% formamide, 5X SSC, 0.1% SDS, 10 μg yeast tRNA, 10 μg poly A RNA, 1 μg human COT-1 DNA). Immediately prior to hybridization, the microarrays were prehybridized in a solution of 5X SSC, 1% SDS, and 1% BSA at 55°C for 45 min. After prehybridization, the arrays were vigorously washed in ddH₂O to remove all traces of the prehybridization solution, rinsed in isopropanol, and dried at room temperature. The samples were denatured at 95°C for 2 min and placed on the prehybridized arrays, covered with Lifterslip coverslips (25 mm \times 60 mm, Erie Scientific, Inc., Portsmouth, NH, USA), placed in a hybridization chamber (Corning, Acton, MA, USA) with 30 μl hybridization buffer to maintain humidity, and incubated at 42°C for 16 h in a standard hybridization oven. After hybridization, the arrays were washed in 2X SSC to remove the coverslips, placed in 2X SSC, 0.1% SDS at 55°C with agitation for 5 min, then washed with two successive 5-min washes with 1X SSC and 0.1X SSC at RT. The washed arrays were dried by centrifugation at 50 \times g for 5 min and immediately scanned using a GenePix 4000B microarray scanner (Axon Instruments, Union City, CA, USA).

RNA Samples Used for Microarray Analysis. Total RNA (10 μg , except for the fixed sample) labeled with Cy3 or Cy5 was cohybridized to microarrays. Control RNA was used to facilitate interar-

ray comparisons and was labeled with Cy5. The control RNA was from normal C57BL/6J mouse brain that had been perfused with saline but not fixed or cryoprotected (condition 1). The fixed sample (condition 3) required special treatment. A total of only 1.7 μg was recovered (according to UV absorption measurements), so in order to have balanced fluorescence signals, equal amounts of DNA product after RT (\sim 0.12 μg) were used for the Cy5-labeled sample (condition 1) and for the Cy3-labeled sample (fixed; condition 3). The data was not normalized, and all scatter plots (see Fig. 2) show raw data.

Histological Staining. Tissue samples were cut frozen on a Leica CM3050-S cryostat (Bannockburn, IL, USA). A series of semi-thin sections (50 μm) were stained with Thionine (Nissl stain) and imaged with a Nikon DX1200 (Japan) mounted on an Olympus Macro-AX70 microscope (Melville, NY, USA).

RESULTS

All experimental conditions were performed twice using the same methods (UV absorption measurements, microcapillary electrophoresis, and microarrays) and provided very similar results. Representative results are shown.

RNA Recovery

The amount of RNA extracted from saline-perfused (condition 1), cryoprotected (condition 2), fixed (condition 3), as well as fixed and cryoprotected (condition 4) brains was quantitated using UV absorption measurements. Similar amounts of RNA were extracted from the saline-perfused and cryoprotected specimens (conditions 1 and 2); both with acceptable A_{260}/A_{280} ratios = 1.7 (RNA in water in all conditions). In contrast, RNA recovery from the fixed tissue (condition 3) appeared to be greatly diminished (\sim 0.005% of recovery compared to conditions 1 and 2), with an A_{260}/A_{280} ratio = 1.2, indicating poorer quality RNA. However, when cryoprotection was combined with paraformaldehyde fixation (condition 4), good RNA recovery was again obtained (comparable to the saline-perfused and cryoprotected specimens), with an A_{260}/A_{280} ratio = 1.7.

Integrity of RNA

The Agilent BioAnalyzer was used to investigate further recovery and quality of RNA from cryoprotected, paraformaldehyde-fixed, and fixed and cryoprotected brain compared to saline-perfused brain. The BioAnalyzer assesses recovery and quality of RNA by quantitation of 28S and 18S ribosomal RNA peaks compared to background. The height of the peaks gives an assessment of recovery, whereas the ratio of 28S/18S peaks and background levels give an indication of integrity. The

results of the BioAnalyzer analysis are shown in Fig. 1. Compared to saline-perfused brain (Fig. 1A), RNA recovery from the cryoprotected brain (Fig. 1B) was excellent, with very little degradation and a 28S/18S ratio = 1.35 (vs. a 28S/18S ratio = 1.44 for saline, both good ratios). It is notable that this quality of RNA was obtained even though a total of approximately 2.5 h elapsed between sacrifice and sample freezing. This is consistent with the literature, where it is reported that the quality of RNA from human brains depends on brain pH, a measure of pre-mortem condition, rather than postmortem interval (10–13).

In contrast to the PBS-perfused and cryoprotected tissues (conditions 1 and 2, respectively), RNA from paraformaldehyde-fixed specimens (condition 3) showed significant decreases in recovery compared to the saline-perfused brain (Fig. 1C). In addition, there was evidence for RNA degradation (no peaks detected). These observations are consistent with published reports that used denaturing agarose gel electrophoresis to show that paraformaldehyde treatment decreased both the recovery and quality of RNA extracted from brain (14–17).

Unexpectedly, brains that were cryoprotected after 4% paraformaldehyde perfusion (condition 4) showed excellent RNA recovery. The yield of the RNA was comparable to brains perfused with saline solution only or cryoprotected only (not fixed) (conditions 1 and 2), with a 28S/18S ratio = 1.15 and only a little higher degradation as shown by the Agilent Bioanalyzer result (Fig. 1D).

Microarray Analysis of Brain RNA

One possible explanation for the unexpected results concerning recovery of RNA from fixed tissues is that paraformaldehyde is a cross-linking agent, and the cross-linked RNA may not be able to enter agarose gels or the Agilent BioAnalyzer. This would give the incorrect impression of diminished recovery and/or degradation, which was the explanation provided in the literature (14–16). Consistent with the notion that paraformaldehyde cross-links but does not degrade RNA, this fixation method is commonly employed for *in situ* hybridization and does not seem to appreciably degrade RNA in that setting.

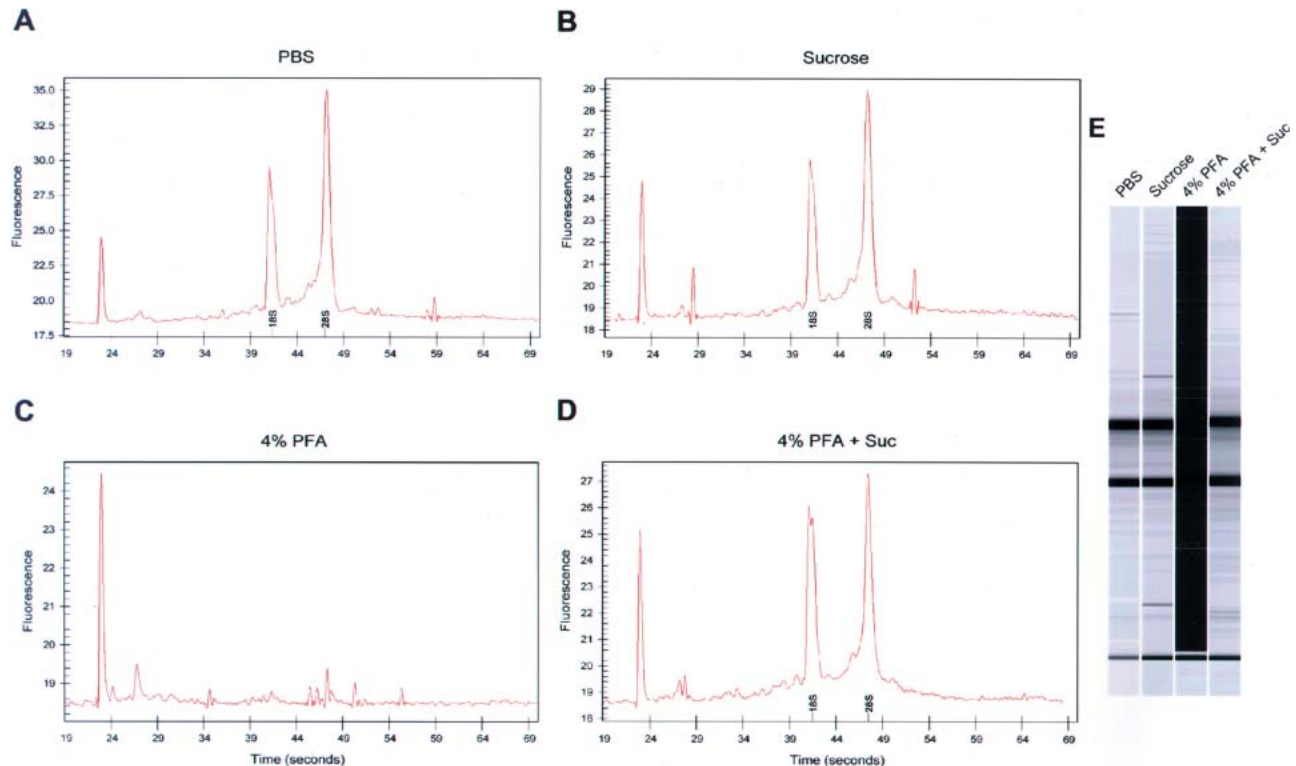


Fig. 1. Recovery and quality of brain RNA assessed using the Agilent BioAnalyzer 2100. (A) Saline-perfused brain (PBS) (condition 1). (B) Saline-perfused and cryoprotected (sucrose-perfused) brain (condition 2). (C) Saline-perfused and 4% paraformaldehyde (PFA)-fixed brain (condition 3). (D) Saline-perfused, 4% PFA-fixed, and cryoprotected (sucrose-perfused) brain (condition 4). (E) Gel-like display of Agilent Bioanalyzer 2100 results for all samples.

As a test independent of gel electrophoresis or the BioAnalyzer, a microarray analysis of RNA recovered from the four types of brain sample was performed. The results are shown in Fig. 2. One experiment compared Cy3-labeled cryoprotected brain RNA to Cy5-labeled saline-perfused brain RNA. A log–log scatter plot comparing the two channels displayed excellent linearity (Fig. 2A). In addition, the average signal-to-noise ratio for both channels was comparable (3.2 ± 0.9 for Cy5, 3.8 ± 1.1 for Cy3). Another experiment compared paraformaldehyde-fixed brain labeled with Cy3 to saline-perfused brain RNA labeled with Cy5 (Fig. 2B). Though the recovery and quality of RNA used for the fixed brain channel was greatly diminished as judged using UV absorption measurements and the BioAnalyzer, log–log scatter plots displayed good linearity except for a perceptible bias at lower intensities (Fig. 2B). The average signal-to-noise ratio was again comparable for both channels (3.1 ± 0.9 for Cy5, 3.4 ± 0.7 for Cy3) despite the fact that only $1.7 \mu\text{g}$ of RNA was nominally used for the fixed brain RNA channel (Cy3). The signal-to-noise ratio for the paraformaldehyde channel was thus much better than would be expected from the UV absorption measurements or Bioanalyzer results. Finally, RNA from the brain that was fixed and cryoprotected (Cy3) compared to PBS-perfused brain RNA (Cy5) showed good results, with similar average signal–noise ratio for both channels (3.2 ± 0.8 for Cy5, 3.8 ± 1.2 for Cy3) and good linearity in a log–log scatter plot (Fig. 2C).

Histological Staining

In order to assess histological quality, sections cut from brains that underwent the complete perfusion protocol (saline, paraformaldehyde, and cryoprotection; condition 4) were stained for neuronal cell bodies according to the Nissl method (Fig. 3). Microscopic inspection of the section revealed excellent morphology and differentiation of the stain. Neuroanatomical territories classically revealed by the Nissl stain were clearly delineated. There was no appreciable difference between the material that was cut frozen immediately after perfusion and that which underwent the canonical histological preparation where specimens were allowed to post-fix in paraformaldehyde and sink in 30% sucrose (note that the specimen sinks in the cryoprotecting solution when the tissue is saturated).

DISCUSSION

In this report, we examined the use of paraformaldehyde fixation and cryoprotection as techniques to help registration of harvested voxels with neuroanatomy.

Compared to saline-perfused brain, cryopreservation did not result in any appreciable decrease in RNA recovery or quality. This was demonstrated by UV absorption measurements, BioAnalyzer data, and signal-to-noise ratios obtained from a 22,172 cDNA microarray. In contrast, paraformaldehyde fixation greatly reduced both the yield and the integrity of recovered RNA as judged by UV absorption and the Bioanalyzer. But when analyzed using a microarray, it was found that the paraformaldehyde-fixed samples still retained much more signal than would have been expected. The apparently misleading reduction in the amount of RNA from fixed brain as judged by UV absorption and the Bioanalyzer may be a consequence of RNA cross-linking by the paraformaldehyde. This cross-linked RNA would fail to enter a gel matrix such as that used by the Bioanalyzer and would give the erroneous impression of degraded RNA. This point of view was in fact advanced by studies described in the literature that assessed integrity of RNA from fixed tissues using agarose gel electrophoresis (14–17). However, the microarray data reported here suggests that the RNA is not degraded by the paraformaldehyde fixation but remains intact and can be labeled for analytic purposes. These observations are consistent with the fact that paraformaldehyde fixation is routinely employed for *in situ* hybridization.

The combination of buffered saline, paraformaldehyde, and sucrose perfusion appeared to yield very good results in terms of RNA quality as compared to brain samples that had only been fixed. These observations suggest that the sucrose gradient perfusion helped recover the RNA signal from the paraformaldehyde-fixed tissue as judged by UV absorption and the Bioanalyzer and is consistent with the idea that the RNA is not largely degraded by the paraformaldehyde fixation.

As the resolution of voxellation is improved, registration between the underlying neuroanatomy and the harvested voxels will become increasingly important. At lower levels of resolution, visual inspection of fresh or fresh-frozen sections is sufficient. However, the inherent low contrast of these specimens makes it difficult to identify boundaries between structures of small size or subtly different microscopic anatomy. Two factors that can improve neuroanatomical labeling of harvested voxels include cryopreservation and fixation. Both processes improve the resilience and integrity of brain slices and help minimize deformation during voxellation. Crucially, proper use of these methods also allows the use of histological stains to improve contrast in the voxelated section. Methods already exist for histological staining of tissue compatible with recovery of RNA for gene expression profiling (18). Aldehyde

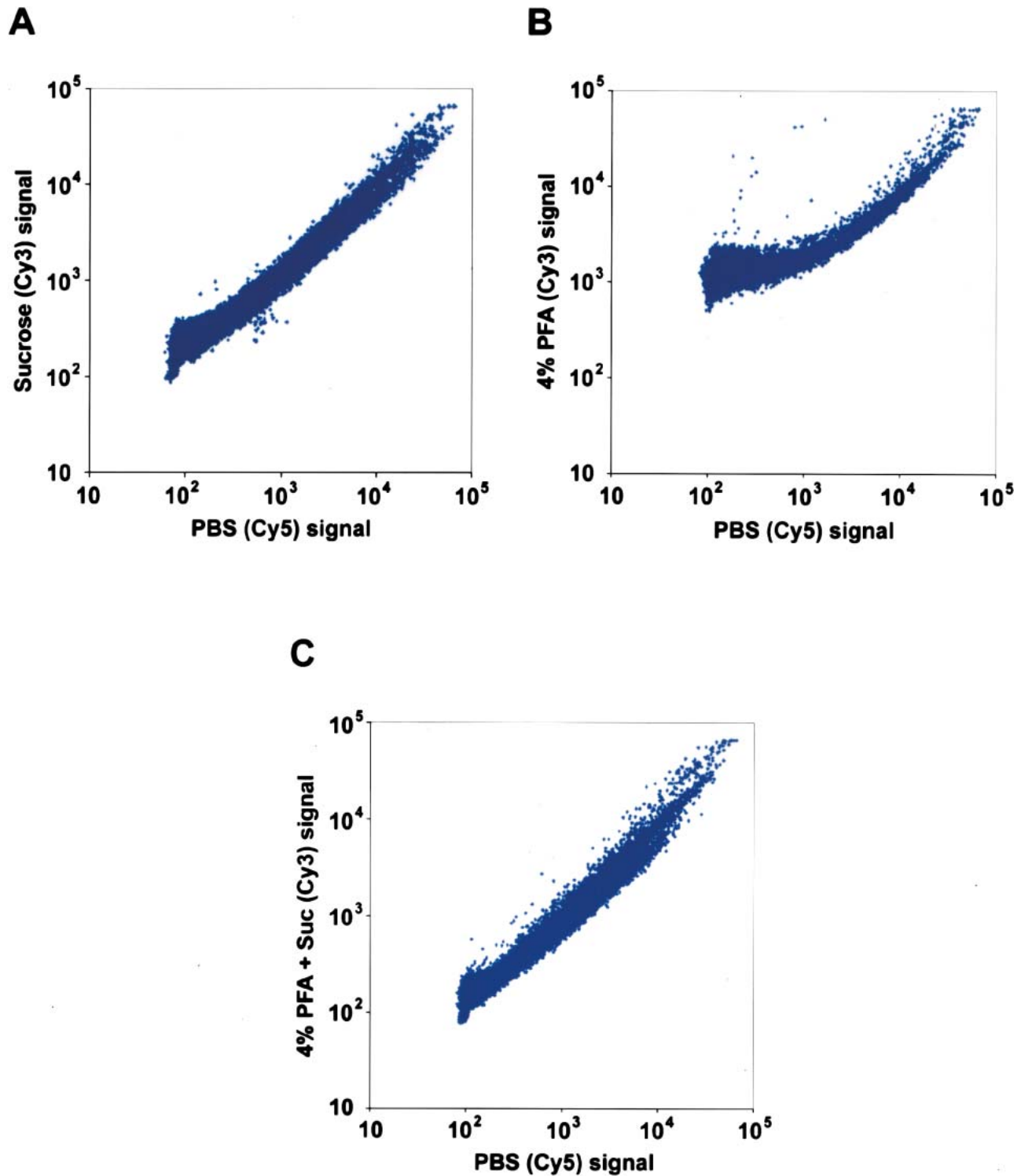


Fig. 2. Comparing transcript profiles from saline-perfused, cryoprotected, paraformaldehyde-fixed, and paraformaldehyde-fixed and cryoprotected brain. (A) Comparison of transcript profiles from cryoprotected brain (Cy3) and saline-perfused brain (Cy5). (B) Comparison of transcript profiles from paraformaldehyde-fixed brain (Cy3) and saline-perfused brain (Cy5). (C) Comparison of transcript profiles from paraformaldehyde-fixed and cryoprotected brain (Cy3) and saline-perfused brain (Cy5).

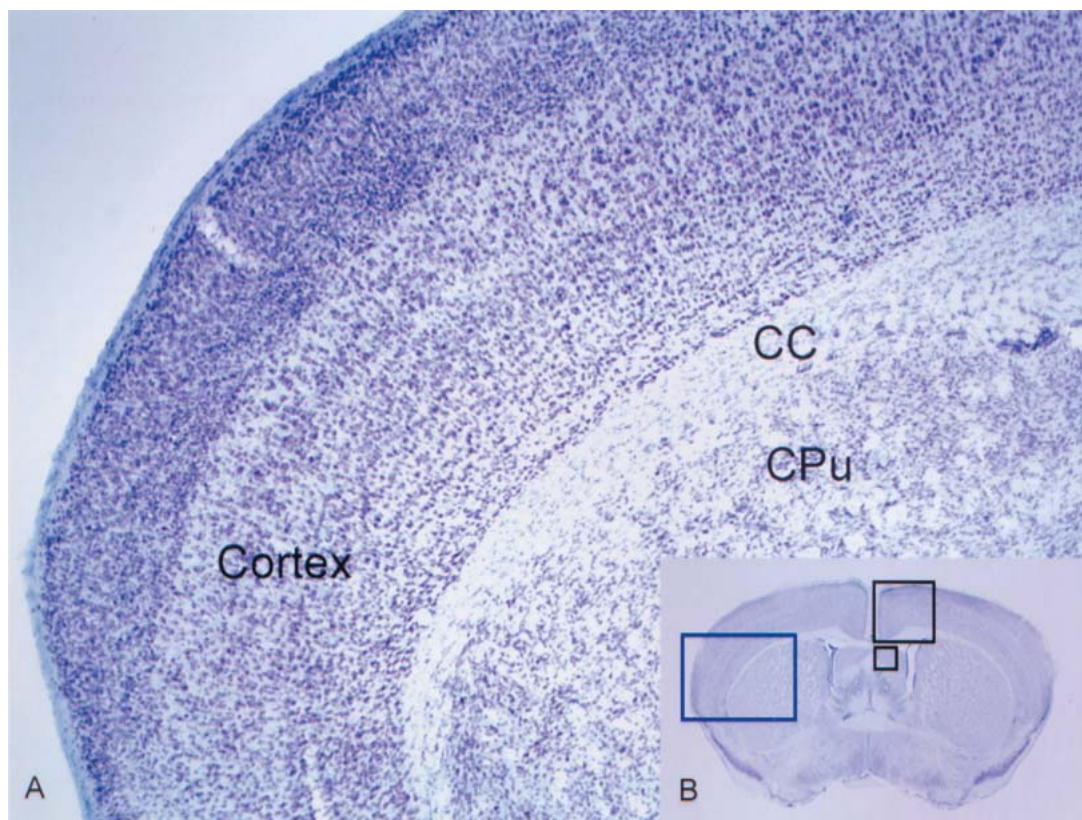


Fig. 3. Histology. (A) Detail of a coronal section from paraformaldehyde-fixed, cryoprotected, and Nissl-stained mouse brain. Note the excellent differentiation of the stain in the cortex that allows discrimination of cortical layers (CC = corpus callosum; CPu = caudate-putamen). (B) Localization of the selected region showing the boundaries of several neuroanatomical structures (blue rectangle). A relative size comparison of low (7.5 μ l) and high (1 μ l) resolution voxels is indicated (black squares).

fixation and cryoprotection should afford the use of a wider variety of histological stains to permit resolution of finer neuroanatomical detail.

In conclusion, our results indicate that the optimal strategy for obtaining good-quality RNA and anatomical information from voxelation is to use both paraformaldehyde fixation and cryopreservation complemented by histological staining to increase contrast and to provide a robust template for neuroanatomical segmentation.

ACKNOWLEDGMENTS

This work was supported by NIH/NIDA (Nos. DA015802, DA05010), NARSAD Young Investigator Award, Tobacco-Related Disease Research Program (No. 11RT-0172), and Alzheimer's Association (No. IIRG-02-3609) grants to D. J. S.; and by NIH/NLM (No. 5 R01 LM05639), NIH/NCRR (No. P41 RR13642), and NIH/NIMH (No. P20 MH65166 and P01 MH52176) grants to A. W. T. The authors wish to thank Yi Ding at the Laboratory of Neuro Imaging for her assistance during perfusion and histological processing.

REFERENCES

1. Liu, D. and Smith, D. J. 2003. Voxelation and gene expression tomography for the acquisition of 3-D gene expression maps in the brain. *Methods* 31:317–325.
2. Singh, R. P. and Smith, D. J. 2003. Genome scale mapping of brain gene expression. *Biol. Psychiatry* 53:1069–1074.
3. Brown, V. M., Ossadtchi, A., Khan, A. H., Yee, S., Laca, G., Melega, W. P., Cherry, S. R., Leahy, R. M., and Smith, D. J. 2002. Multiplex three-dimensional brain gene expression mapping in a mouse model of Parkinson's disease. *Genome Res.* 12:868–884.
4. Brown, V. M., Ossadtchi, A., Khan, A. H., Cherry, S. R., Leahy, R. M., and Smith, D. J. 2002. High-throughput imaging of brain gene expression. *Genome Res.* 12:244–254.
5. Ossadtchi, A., Brown, V. M., Khan, A. H., Cherry, S. R., Nichols, T. E., Leahy, R. M., and Smith, D. J. 2002. Statistical analysis of multiplex brain gene expression images. *Neurochem. Res.* 27: 1113–1121.
6. Singh, R. P., Brown, V. M., Chaudhari, A., Khan, A. H., Ossadtchi, A., Sforza, D. M., Meadors, A. K., Cherry, S. R., Leahy, R. M., and Smith, D. J. 2003. High-resolution voxelation mapping of human and rodent brain gene expression. *J. Neurosci. Methods* 125:93–101.
7. Anness, J. and Toga, W. A. 2002. Postmortem anatomy. Pages 537–571, in Toga, A. W. and Mazziotta, J. C. (eds.), *Brain mapping: the methods*, Academic Press, New York.

8. Rosene, D. L. and Rhodes, K. J. 1990. Cryoprotection and freezing methods to control ice crystal artifact in frozen sections of fixed and unfixed brain tissue. Pages 360–390, in Conn, P. M. (ed.), *Quantitative and qualitative microscopy*, Academic Press, New York.
9. Hegde, P., Qi, R., Abernathy, K., Gay, C., Dharap, S., Gaspard, R., Hughes, J. E., Snesrud, E., Lee, N., and Quackenbush, J. 2000. A concise guide to cDNA microarray analysis. *Biotechniques* 29: 548–562.
10. Harrison, P. J., Heath, P. R., Eastwood, S. L., Burnet, P. W., McDonald, B., and Pearson, R. C. 1995. The relative importance of premortem acidosis and postmortem interval for human brain gene expression studies: selective mRNA vulnerability and comparison with their encoded proteins. *Neurosci. Lett.* 200: 151–154.
11. Goss, J. R., Finch, C. E., and Morgan, D. G. 1990. GFAP RNA increases during a wasting state in old mice. *Exp. Neurol.* 108:266–268.
12. Johnson, S. A., Morgan, D. G., and Finch, C. E. 1986. Extensive postmortem stability of RNA from rat and human brain. *J. Neurosci. Res.* 16:267–280.
13. Bahn, S., Augood, S. J., Ryan, M., Standaert, D. G., Starkey, M., and Emson, P. C. 2001. Gene expression profiling in the post-mortem human brain—no cause for dismay. *J. Chem. Neuroanat.* 22:79–94.
14. Parlato, R., Rosica, A., Cuccurullo, V., Mansi, L., Macchia, P., Owens, J. D., Mushinski, J. F., De Felice, M., Bonner, R. F., and Di Lauro, R. 2002. A preservation method that allows recovery of intact RNA from tissues dissected by laser capture microdissection. *Anal. Biochem.* 300:139–145.
15. Scheidl, S. J., Nilsson, S., Kalen, M., Hellstrom, M., Takemoto, M., Hakansson, J., and Lindahl, P. 2002. mRNA expression profiling of laser microbeam microdissected cells from slender embryonic structures. *Am. J. Pathol.* 160:801–813.
16. Goldsworthy, S. M., Stockton, P. S., Trempus, C. S., Foley, J. F., and Maronpot, R. R. 1999. Effects of fixation on RNA extraction and amplification from laser capture microdissected tissue. *Mol. Carcinog.* 25:86–91.
17. Van Deerlin, V. M. D., Ginsberg, S. D., Lee, V. M. Y., and Trojanowski, J. Q. 2002. The use of fixed human post mortem brain tissue to study mRNA expression in neurodegenerative diseases: applications of microdissection and mRNA amplification. Pages 201–235, in Geshwind, D. H. and Gregg, J. P. (eds.), *Microarrays for the neurosciences: an essential guide*, MIT Press, Boston.
18. Bonaventure, P., Guo, H., Tian, B., Liu, X., Bittner, A., Roland, B., Salunga, R., Ma, X. J., Kamme, F., Meurers, B., Bakker, M., Jurzak, M., Leyson, J. E., and Erlander, M. G. 2002. Nuclei and subnuclei gene expression profiling in mammalian brain. *Brain Res.* 943:38–47.